Title

Enhancing Aqueous Chlorate Reduction Using Vanadium Redox Cycles and pH Control.

Authors

Gao, Jinyu

Chen, Gongde

Fu, Qi

et al.

Publication Date

2023-11-17

DOI

10.1021/acs.est.3c06519

Peer reviewed

Environmental Science & Technology

pubs.acs.org/est

Article

Enhancing Aqueous Chlorate Reduction Using Vanadium Redox Cycles and pH Control

Jinyu Gao,* Gongde Chen, Qi Fu, Changxu Ren, Cheng Tan, Haizhou Liu, Yin Wang, and Jinyong Liu*

Cite This: *Environ. Sci. Technol.* 2023, 57, 20392−20399

Read Online

ACCESS | Metrics & More | Article Recommendations | Supporting Information

ABSTRACT: Chlorate (ClO_3^-) is a toxic oxyanion pollutant from industrial wastes, agricultural applications, drinking water disinfection, and wastewater treatment. Catalytic reduction of ClO_3^- using palladium (Pd) nanoparticle catalysts exhibited sluggish kinetics. This work demonstrates an 18-fold activity enhancement by integrating earth-abundant vanadium (V) into the common Pd/C catalyst. X-ray photoelectron spectroscopy and electrochemical studies indicated that V^V and V^{IV} precursors are reduced to V^{III} in the aqueous phase (rather than immobilized on the carbon support) by Pd-activated H_2. The $V^{III/IV}$ redox cycle is the predominant mechanism for the ClO_3^- reduction. Further reduction of chlorine intermediates to Cl^- could proceed via $V^{III/IV}$ and $V^{IV/V}$ redox cycles or direct reduction by Pd/C. To capture the potentially toxic V metal from the treated solution, we adjusted the pH from 3 to 8 after the reaction, which completely immobilized V^{III} onto Pd/C for catalyst recycling. The enhanced performance of reductive catalysis using a Group 5 metal adds to the diversity of transition metals (e.g., Cr, Mo, Re, Fe, and Ru in Groups 6−8) for water pollutant treatment via various unique mechanisms.

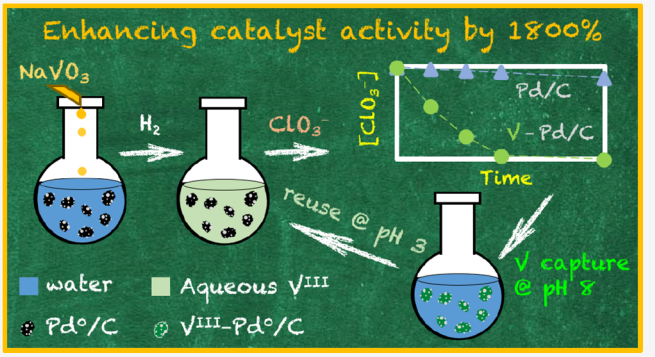

KEYWORDS: *vanadium, palladium, catalyst, chlorate, X-ray photoelectron spectroscopy (XPS), electrochemical study, redox, recycle*

INTRODUCTION

The global annual production of sodium chlorate ($NaClO_3$) has exceeded 4 million tons for pulp and paper bleaching, pyrotechnics, weed control, and various other applications.[1] ClO_3^- is also a common byproduct from drinking water disinfection using NaClO or ClO_2[2] and wastewater treatment with electrochemical[3,4] or photochemical processes.[5,6] Upon entering the environment, ClO_3^- can adversely affect ecosystems. For instance, it exhibits high toxicity toward specific algal species in aquatic environments[7] and can potentially suppress the nitrification process in soil.[8] Human exposure to ClO_3^- through drinking water, dairy supply chain, and agricultural products can lead to various health effects, including thyroid dysfunction and methemoglobinemia.[9] The World Health Organization,[10] European Union (EU),[11] and China[12] have established the drinking water limit of 0.7 mg L^{-1} for ClO_3^-, while the United States has set a health reference level of 0.21 mg L^{-1}, with a minimum reporting level of 0.02 mg L^{-1}.[13,14] Additionally, undesired formation of ClO_3^- also takes place in both essential and emerging electrochemical processes such as chloralkali,[15,16] water splitting,[17] and seawater valorization.[18] Thus, technological advances in chlorate reduction hold immense importance across various fields.

The exploration of platinum group metals (PGM) as catalysts for aqueous ClO_3^- reduction has been ongoing since the early 1990s.[19] While PGM nanoparticles catalyze the clean reduction of ClO_3^- by H_2 into Cl^- and H_2O (eq 1), they typically demonstrate limited activity, necessitating high catalyst loadings.[20−25]

$$ClO_3^- + 3H_2 \rightarrow Cl^- + 3H_2O \quad (1)$$

Previously, we have enhanced the reduction of oxyanions by incorporating Group 6−8 transition metals into PGM catalysts.[26−29] Each secondary metal imparts novel and unique functionalities. For instance, $Cr(OH)_3$ formed in various PGM catalysts (e.g., Pd or Rh nanoparticles supported by carbon, alumina, or silica) remarkably enhanced the adsorption of oxyanions.[28] The reduced Mo and Re oxide species on the PGM catalysts substantially accelerated oxyanion reduction via $Mo^{IV/VI}$ and $Re^{V/VII}$ redox cycles, respectively.[27,30] The immobilization of Ru^0 nanoparticles onto Pd/C or Rh/C

Received: August 11, 2023
Revised: October 26, 2023
Accepted: October 27, 2023
Published: November 17, 2023

https://doi.org/10.1021/acs.est.3c06519
Environ. Sci. Technol. 2023, 57, 20392−20399

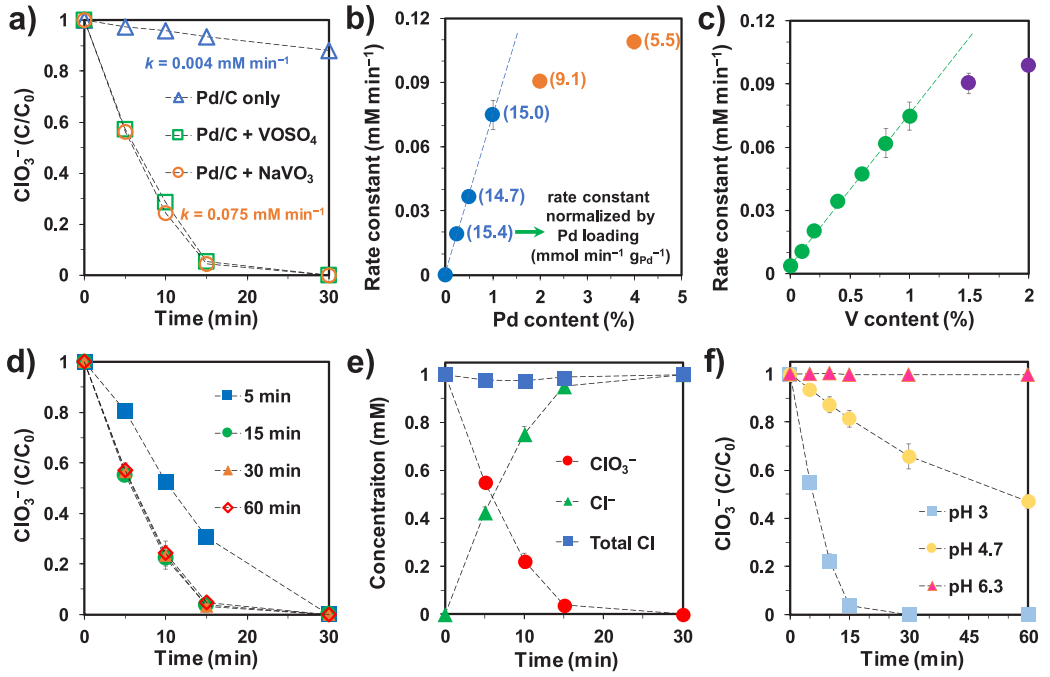

Figure 1. (a) Time profiles of ClO_3^- reduction by Pd/C added with V^V and V^{IV} precursors, relationships between ClO_3^- reduction rate constants and (b) Pd and (c) V contents of the catalysts, (d) time profiles of ClO_3^- reduction with V−Pd/C catalysts prepared by allowing various time intervals between adding $NaVO_3$ under H_2 and adding ClO_3^-, (e) chlorine balance during ClO_3^- reduction, and (f) time profiles of ClO_3^- reduction by V−Pd/C at various pH. Unless specified, all reactions used 0.5 g L^{-1} 1 wt % V−1 wt % Pd/C, 1 mM ClO_3^-, pH 3.0, 1 atm H_2, and 20 °C.

initiated a synergistic working mode, in which Ru rapidly reduces ClO_3^- while Pd or Rh scavenges the Ru-passivating chlorine intermediates.[29] We were thus motivated by extending the exploration to Group 5 metals.

Vanadium (V) is renowned for its easy accessibility to four adjacent oxidation states ranging from +2 to +5. This feature makes V a versatile redox catalyst and an active participant in various chemical and electrochemical processes.[31−33] V is also attractive for application because it is the sixth most abundant element among the transition metals and the 20th most abundant element overall in the Earth's crust.[34] Particularly for environmental application scenarios, V is found in various natural and polluted waters.[35−38] In this study, by leveraging the redox property of V and integrating it with a common Pd/C catalyst, we substantially accelerated the reduction of aqueous ClO_3^-. In contrast to Group 6−8 metals, V exhibits distinct behavior by serving as an electron shuttle in the aqueous phase for ClO_3^- reduction. After the reaction, reduced V^{III} can be readily immobilized on Pd/C through pH adjustment. This work shows that simple chemical innovations can substantially enhance the catalyst activity and effectively capture the potentially harmful metal species.

MATERIALS AND METHODS

General Information. Ultrahigh-purity H_2 gas (99.999%) was supplied by Airgas. Activated carbon (no. L11860) for Pd/C preparation, $NaVO_3$, $VOSO_4$, and V_2O_3 were used as received from Alfa Aesar. $NaClO_3$ and Na_2PdCl_4 were purchased from Sigma-Aldrich. All aqueous solutions were prepared with 18.2 MΩ cm^{-1} Milli-Q water. The Pd/C catalyst was prepared using our recently developed all-*in situ* method, which has been validated in our previous studies.[28,29,39,40] Specifically, a magnetic stir bar, 40 mg of activated carbon, 400 mL of DI water, and the desired amount of Na_2PdCl_4 (dissolved in a stock solution) were sequentially placed in a 500 mL round-bottom flask. The flask was capped with a rubber stopper and sonicated for 1 min. Next, the suspension was stirred at 350 rpm for 5 min to facilitate the adsorption of Pd^{II} onto the carbon support. The suspension was then sparged with 1 atm H_2 for 5 min at room temperature to reduce adsorbed Pd^{II} to Pd^0 on the carbon support. The H_2 gas was introduced through a 16 gauge stainless-steel needle penetrating the stopper. Another needle served as the sampling port and the gas outlet to a fume hood. The solid catalyst was collected on filter paper in air, dried by airflow in the fume hood, and used for the subsequent steps.

Catalytic ClO_3^- Reduction. In a 50 mL round-bottom flask, 25 mg of Pd/C and the desired amount of the V precursor ($NaVO_3$ or $VOSO_4$, dissolved in a stock solution) were mixed together with 50 mL of Milli-Q water. The solution pH was adjusted to 3.0 with 1 N (i.e., 0.5 M) H_2SO_4. The mixture was stirred under H_2 sparging for 15 min to ensure the complete reduction of the V precursor to lower oxidation states. Once the V reduction was complete, $NaClO_3$ was added to the flask to initiate the reaction. Aliquots were collected periodically and filtered using a 0.22 μm cellulose membrane. The ClO_3^- and Cl^- in the aliquots were quantified using a Dionex ICS-5000 ion chromatography (IC) with a conductivity detector. The anions were separated using an IonPac AS19 column at 30 °C, with a 20 mM KOH eluent at 1 mL min^{-1}. The dissolved V in the aqueous phase was monitored by inductively coupled plasma-mass spectroscopy (ICP-MS, Agilent 7700 series).

Characterization of Pd/C-Reduced Vanadium Species. After the $NaVO_3$ addition to the Pd/C suspension and 15 min of H_2 sparging, the mixture was promptly transferred to

https://doi.org/10.1021/acs.est.3c06519
Environ. Sci. Technol. 2023, 57, 20392−20399

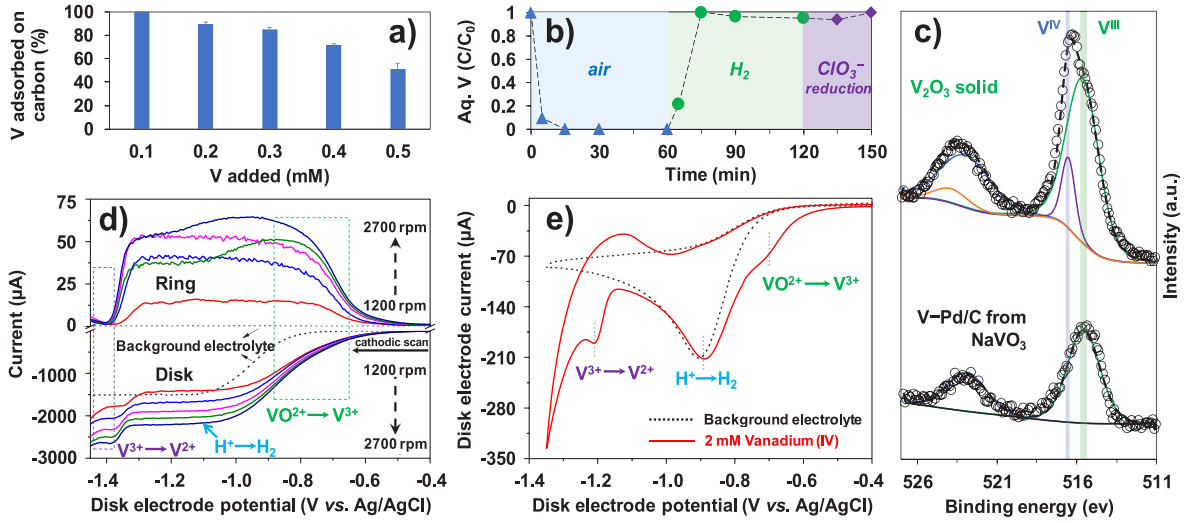

Figure 2. (a) Fraction of V^V adsorbed on Pd/C (0.5 g L^{-1}, 1 wt % V^V if fully adsorbed), (b) aqueous V concentration after adding $NaVO_3$ (5 mg L^{-1} as V) into the Pd/C suspension under varying conditions, (c) V 2p XPS spectra of the $V^{III}{}_2O_3$ reference and V–Pd/C prepared from $NaVO_3$, and (d) linear sweep voltammetry of $V^{IV}O^{2+}$ on an RDDE with a scan rate of 50 mV s^{-1}. The ring electrode potential was fixed at 0.8 V. Dashed lines represent the linear sweep voltammetry of the background electrolyte at 50 mV s^{-1} and 2700 rpm; (e) cyclic voltammetry of $V^{IV}O^{2+}$ on a gold disk electrode. Dashed lines represent the voltammograms of the background electrolyte at 50 mV s^{-1}. Cyclic scan on the electrode started in the cathodic direction followed by the anodic direction. Other electrochemical study conditions for (d) and (e): 2 mM $VOSO_4$, 0.5 M Na_2SO_4, 1.5 M ionic strength, and pH 3.0.

an anaerobic glovebag (98% N_2, 2% H_2; Coy Laboratories). The ICP-MS analysis indicated limited adsorption of V by Pd/C after H_2 exposure (see Results and Discussion). To facilitate X-ray photoelectron spectroscopy (XPS) characterization, the dissolved V was forced to be immobilized on Pd/C by evaporating the water at 110 °C (sand bath) within the glovebag. The dried powder was mixed with TiO_2 (as an internal standard with the Ti $2p_{3/2}$ binding energy (BE) of 458.7 eV). The mixture was loaded onto copper conductive tape and placed inside an anaerobic tube. The tube was transferred into a glovebox connected to an XPS instrument (AXIS Supra Kratos Analytical) equipped with a monochromatized Al Kα source. Inside the glovebox, the sample was retrieved from the tube and directly loaded into the instrument for characterization. The XPS spectra were fitted using CasaXPS software (version 2.3.19), with constrained separations of spin–orbit coupling doublet peaks (7.33 eV for V 2p, 5.76 eV for Ti 2p, and 5.27 eV for Pd 3d) and constrained ratios of the doublet peak areas (2:1 for V and Ti 2p and 3:2 for Pd 3d).

To gain further insights into aqueous V speciation under the reducing environment by H_2–Pd/C, we employed a combination of rotating ring-disk electrode (RRDE) techniques and static cyclic voltammetry (CV) to characterize the oxidation states of V species at various reduction potentials. We used a three-electrode system, which included a gold RRDE working electrode, a platinum counter electrode, and a Ag/AgCl reference electrode, following a previously established procedure.[41] The electrochemical experiments were performed using $NaVO_3$ and $VOSO_4$ solutions at pH 3.0 (the same pH for ClO_3^- reduction), with 0.5 M Na_2SO_4 as the background electrolyte. Prior to the experiments, the V precursor solutions underwent a 30 min purge with N_2 gas to remove dissolved O_2. Throughout the experiments, a continuous flow of N_2 gas was maintained above the solution to prevent the ingress of O_2. In the CV experiments, the disk electrode potential was scanned over the range from +0.40 to −1.35 V, with the scan rate ranging from 25 to 200 mV s^{-1}. The disk current was recorded. In the RRDE study, the potential of the disk electrode was scanned within a targeted range, while the ring electrode potential remained fixed at a specific value. The rotating speed of the ring-disk electrode ranged from 400 to 2700 rpm. Both the disk and ring currents were recorded. Details regarding the assignment of V reduction peaks in the voltammograms are provided in Text S1 of the Supporting Information.

RESULTS AND DISCUSSION

Vanadium Substantially Enhances ClO_3^- Reduction. The addition of either a V^V ($NaVO_3$) or V^{IV} ($VOSO_4$) precursor to Pd/C substantially enhanced ClO_3^- reduction by 18-fold compared to bare Pd/C, with both precursors exhibiting equal activity (Figure 1a and Figure S1). At pH 3.0 and 20 °C, the 1 wt % V–1 wt % Pd/C catalyst at 0.5 g L^{-1} accomplished >99.9% reduction of 1 mM ClO_3^- within 0.5 h. We postulated that Pd/C could potentially reduce V^V and V^{IV} to the same active species (i.e., V^{III} or V^{II}, characterized in the next section) for ClO_3^- reduction. NaV^VO_3 was used as the catalyst precursor for further studies. To optimize the catalyst formula, we investigated how the varying Pd and V contents affect ClO_3^- reduction activity using our recently developed method, which allows for the "instant" preparation of Pd/C with any metal content.[39] By maintaining a constant V content of 1 wt %, we observed that the increasing Pd content raised the apparent rate constant (Figure 1b). However, surpassing 1 wt % Pd did not result in a proportional acceleration of ClO_3^- reduction. In fact, the rate constant normalized by the total Pd mass decreased, most likely due to decreased Pd dispersion.[29,39] Notably, no ClO_3^- reduction was observed when Pd was absent (i.e., carbon only, Figure 1b), indicating the role of Pd nanoparticles in harnessing electrons from H_2.

When the Pd content was fixed at 1 wt % and the V content was progressively increased from 0 to 1 wt %, we observed a proportional increase in the reaction rate. However, beyond 1

https://doi.org/10.1021/acs.est.3c06519
Environ. Sci. Technol. 2023, 57, 20392−20399

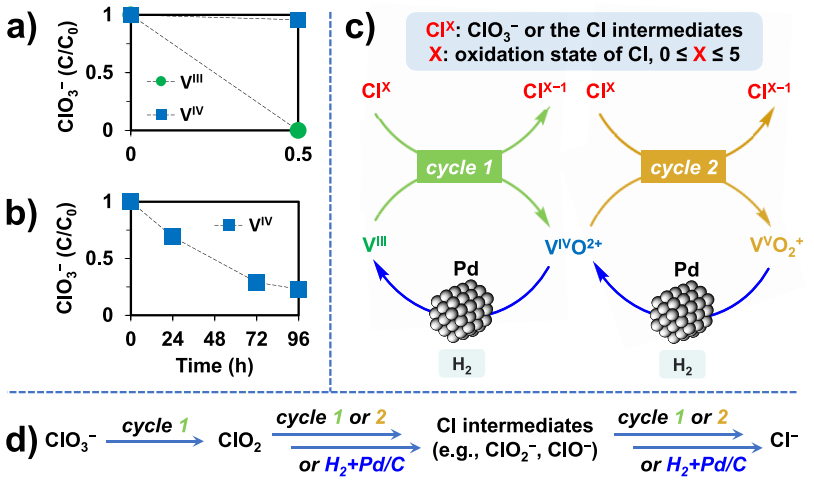

Figure 3. (a,b) Time profiles for 0.1 mM ClO_3^- reduction by 1 mM V^{III} and V^{IV}, (c) proposed catalytic cycles for the reduction of ClO_3^- and the reaction intermediates, and (d) overall reaction pathway for the reduction of ClO_3^- to Cl^-.

wt % V, a disproportional acceleration in ClO_3^- reduction was observed (Figure 1c). For the subsequent studies, we used 1 wt % for both Pd and V. The highest ClO_3^- reduction activity was observed when V^V–Pd/C was exposed to H_2 for 15 min or longer before adding ClO_3^- (Figure 1d). Shorter H_2 exposure (e.g., 5 min) led to a slower reaction. Hence, the reduction of V^V by Pd-activated H_2 is crucial for ClO_3^- reduction, and it can be achieved within 15 min at ambient pressure and temperature.

The V–Pd/C ranks among the top-tier catalysts in terms of the ClO_3^- reduction rate (Table S1). The only catalyst known to exhibit greater activity is our previously reported Ru–Pd/C.[29] However, V is a much more earth-abundant and readily available metal than Ru. V^V oxyanions are commonly found in natural waters[35−38] and may enhance catalysis. A good mass balance was observed between ClO_3^- and Cl^-, indicating that ClO_3^- was reduced to Cl^- without accumulation of Cl-containing intermediates (Figure 1e). At the challenging ClO_3^- concentrations of 10 and 100 mM, the catalyst exhibited remarkable performance, achieving >99% ClO_3^- reduction within 4 and 8 h, respectively (Figure S2). We also evaluated the performance of V–Pd/C in synthetic brines containing 2 M Cl^- and 1 M SO_4^- ions, respectively. Despite the observed activity loss in both scenarios, ClO_3^- reduction still completed within 4 h (Figure S3). Thus, V–Pd/C can be potentially applied to treat concentrated ClO_3^- under specific scenarios. The activity of V–Pd/C was pH-dependent with faster reactions at lower pH (Figure 1f). Similar trends have been observed from Re–Pd/C and Mo–Pd/C catalysts.[27,30,42] The proton can facilitate electron transfer in the deoxygenation of V-coordinated ClO_3^-[27,30,42] and the reduction of the V site to lower oxidation states.[43,44]

Characterization of Reduced Vanadium Species. ICP-MS analysis revealed that Pd/C had a limited adsorption capacity for V^V (Figure 2a). When 1 wt % V^V (corresponding to 0.1 mM in solution versus 0.5 g L^{-1} Pd/C) was added, it was fully adsorbed by Pd/C. However, after a brief H_2 exposure, most adsorbed V was released into solution again (Figure 2b). Thus, the reduced V species could not be readily immobilized on Pd/C. To characterize the prevailing oxidation states of V in the H_2+Pd/C system, we evaporated the water at 110 °C in an anaerobic glovebag and forced V to deposit on the Pd/C powder. XPS analysis observed the V $2p_{3/2}$ BE at 515.6 eV (Figure 2c), which is consistent with the previously reported V^{III}.[45] The BE value also matched the major peak BE at 515.6 eV of the $V^{III}_2O_3$ standard (a minor BE peak at 516.5 eV corresponded to V^{IV} due to oxidation).[46] Therefore, the V^V precursor was reduced by H_2+Pd/C to V^{III}. XPS also confirmed metallic Pd^0 ($3d_{5/2}$ BE of 335.44 eV, Figure S4) under the H_2 atmosphere.

To corroborate the XPS results, we used an electrochemical method to investigate the oxidation state of aqueous V after reduction. To simulate the H_2+Pd/C system, V^V was incrementally reduced on an electrode with a potential range that covered the actual redox potential range of the H_2+Pd/C system. The speciation of aqueous V^V varies depending on pH and concentration.[41,47] Visual MINTEQ simulation (Figure S5) suggested that the dominant species was VO_2^+ (93.2%) in our optimized reaction system (pH 3.0 and 1 wt % V, equivalent to 0.1 mM V). The fraction of VO_2^+ decreased as the V concentration increased (Figure S5). To enhance the signal and maintain VO_2^+ as the main species (>90%), we performed the initial electrochemical study at pH 3.0 with a concentration of 0.2 mM NaV^VO_3, which was twice the optimum value. CV and RRDE results demonstrated that the reduction of V^V started at 0.35 V (Figures S6–S9). We analyzed the correlation between peak currents and scan rates in CV and Koutecky–Levich plots (Text S1, Calculation 1).[48] Results showed that V^V underwent one-electron transfer to V^{IV}, predominantly as $V^{IV}O^{2+}$.

However, V^{IV} was not the reactive species responsible for the rapid reduction of ClO_3^- (see evidence in the next section). When we attempted to further reduce V^{IV} at a more negative potential, the low concentration of V (0.2 mM) failed to generate a notable signal due to the pronounced interference from H_2 evolution. Consequently, we used 2 mM $V^{IV}OSO_4$ to further resolve other V species. CV and RRDE analysis (Text S1, Calculation 2) indicated that V^{IV} was initially reduced to V^{III} within the range of −0.78 V to −0.55 V, prior to H_2 evolution, and subsequently reduced to V^{II} at −1.21 V after H_2 evolution (Figure 2d,e). Thus, V^{II} cannot be generated by using H_2 as the reductant. Therefore, V^{III} was the final reduction product from V^V and was responsible for the rapid reduction of ClO_3^-. This is consistent with the XPS characterization.

https://doi.org/10.1021/acs.est.3c06519
Environ. Sci. Technol. 2023, 57, 20392−20399

Vanadium Redox Cycles and ClO_3^- Reduction Mechanisms. Once the V precursor is reduced to V^{III}, it could rapidly reduce ClO_3^-. The reaction between V^{IV} and ClO_3^- could occur, but it was very slow. The homogeneous reaction between $V^{IV}O^{2+}$ (1 mM) and ClO_3^- (0.1 mM) was negligible within 0.5 h (Figure 3a,b), which is the time frame for the complete reduction of 1 mM ClO_3^- using 1 wt % V (0.1 mM)−1 wt % Pd/C (0.5 g L^{-1}, Figure 1a). In stark contrast, the homogeneous reaction between 1 mM V^{III} (reduced from V^V by H_2+Pd/C and then separated by filtering off Pd/C) and 0.1 mM ClO_3^- was observed to reach completion within the same time frame (Figure 3a). Given that the reduction of ClO_3^- by bare Pd/C is sluggish (Figure 1a), the activity of V−Pd/C is primarily attributed to V^{III}. According to a previous report, the reaction between V^{III} and ClO_3^- predominantly occurs through one-electron transfer, where V^{III} is oxidized to $V^{IV}O^{2+}$ and ClO_3^- is reduced to ClO_2.[49] Notably, the reported second-order rate constant for ClO_3^- reduction in the previous homogeneous system (pH ∼0 and 20 °C) was 3.2 M^{-1} s^{-1}, lower than that from our V−Pd/C system (15.0 M^{-1} s^{-1} at pH 3 and 20 °C, Figure 1f). This comparison also shows that integration with H_2+Pd/C enables efficient catalysis without highly acidic conditions. The reduction of $V^{IV}O^{2+}$ to V^{III} by H_2+Pd/C completes redox cycle 1 (Figure 3c). V^{III} can also react with ClO_2 and further intermediates (e.g., ClO_2^-, ClO^-, and Cl_2), through one-electron transfer,[49] ultimately to Cl^- (Figures 1e and 3d).

However, the degradation of those intermediates does not solely use V^{III} in cycle 1. First, $V^{IV}O^{2+}$ generated from cycle 1 has substantially higher reactivity with the intermediates compared to ClO_3^-. For example, the rate constants for the reaction of $V^{IV}O^{2+}$ with ClO_2 and ClO^- are 500 and 550 times higher, respectively, than that with ClO_3^-.[49] The reaction of $V^{IV}O^{2+}$ with these intermediates also follows a one-electron transfer mechanism and yields $V^VO_2^+$.[50] The reduction of $V^VO_2^+$ to $V^{IV}O^{2+}$ by H_2+Pd/C closes redox cycle 2 (Figure 3c). Second, it is worth noting that while Pd/C is sluggish in reducing ClO_3^-, it rapidly reduces the intermediates.[29] In summary, the reduction of parent ClO_3^- primarily occurs through cycle 1, yielding ClO_2. The degradation of the intermediates (e.g., ClO_2, ClO_2^-, ClO^-, and Cl_2) can proceed via redox cycle 1 or 2, or they can be directly reduced by Pd/C, eventually generating Cl^- (Figure 3d).

Aqueous Vanadium Capture and Reuse. As mentioned earlier, while 0.1 mM V^V could be completely adsorbed on the Pd/C, V^{III} was released into the aqueous phase during the reaction (Figure 2b). To contain the potentially toxic V species in the catalytic system, we aimed to immobilize V onto carbon after the ClO_3^- reduction. V^{III} readily hydrolyzes[51] and the addition of base (e.g., NH_4OH)[52] can effectively precipitate $V^{III}(OH)_3$. Our Visual MINTEQ simulation found that at pH 8.0, over 99% of V^{III} existed as a $V^{III}(OH)_3$ solid (Figure 4a). We adjusted the solution pH from 3.0 to 8.0 and achieved the rapid and complete immobilization of V^{III} onto Pd/C. To prevent V^{III} oxidation by O_2, pH adjustment and filtration were performed under anaerobic conditions. ICP-MS analysis found that the aqueous V went below the detection limit of 1 μg L^{-1}. Although a small portion of V^{III} may still persist in its hydrolyzed form (e.g., $[V(OH)]^{2+}$, $[V(OH)_2]^+$, and $[V_2(OH)_2]^{4+}$), the increased pH can modify the catalyst surface charge to more negative values,[24] potentially facilitating the adsorption of those cations. After the pH adjustment, we collected the V^{III}−Pd/C solid by filtration. The subsequent redispersion into water at pH 3 resumed the high activity (Figure 4b).

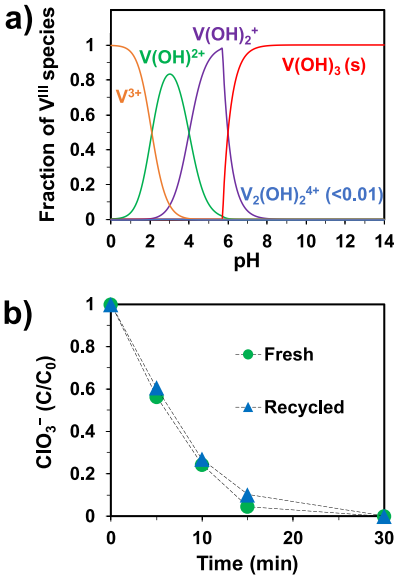

Figure 4. (a) Calculated aqueous V^{III} speciation (5 mg L^{-1} as V, Visual MINTEQ ver. 3.1) and (b) reduction of 1 mM ClO_3^- by fresh and recycled V−Pd/C catalysts. Reaction conditions: 0.5 g L^{-1} 1 wt % V−1 wt % Pd/C, pH 3.0, 1 atm H_2, and 20 °C.

Implications to Catalyst Development for Water Treatment. In the aqueous phase, V precursors (NaV^VO_3 and $V^{IV}OSO_4$) can be efficiently reduced to V^{III} by Pd-activated H_2. The rapid and complete reduction of ClO_3^- is primarily achieved by the redox cycling between V^{III} and $V^{IV}O^{2+}$ as a homogeneous process, but V^{III} can be effectively contained in the catalytic system via pH control. V is naturally present in a diverse range of earth materials[53,54] and can enter the water environment through mechanical and chemical weathering processes.[35,36] The global demand for high-grade steel also keeps releasing V-enriched industrial byproducts into the environment.[37,38,55−57] Therefore, V from either natural or anthropogenic sources in the affected water could accelerate ClO_3^- reduction. In the absence of V cocontaminants, the simple addition of 0.1 mM V can substantially facilitate the reduction of up to 100 mM ClO_3^-. The addition, capture, and recycling of V afford a low-cost and sustainable technical option for ClO_3^- reduction. The reduction and immobilization of V also suggest a novel approach for V removal from water using PGM catalysts and H_2.

Compared to the original Pd/C, the added earth-abundant and low-cost V reduced the amount of expensive Pd/C by 18-fold (Figure 1a) while maintaining the same reaction rate, thus enhancing the cost-effectiveness of the catalyst system. This study demonstrates the great application potential of incorporating redox-active metals to enable new reaction pathways for water pollutant degradation. Our research has investigated various metals in Groups 5 (V), 6 (Cr and Mo), 7 (Re), and 8 (Ru) for enhanced oxyanion reduction with supported PGM catalysts. Each metal follows unique mechanisms through enhancing oxyanion adsorption (e.g., Cr[28]), creation of novel reaction pathways (e.g., V, Mo,[27] and Re[30]), or synergistic work (e.g., Ru[29]). Notably, the reaction pathways created by V, Mo, and Re differ remarkably. V reacts with ClO_3^- through a one-electron transfer process (Figure

https://doi.org/10.1021/acs.est.3c06519
Environ. Sci. Technol. 2023, 57, 20392−20399

3c), whereas Mo and Re oxometallates reduce ClO_3^- via oxygen atom transfer (eqs 2 and 3).

$$ClO_x^- + Mo^{IV}O_y \rightarrow ClO_{x-1}^- + Mo^{VI}O_{y+1} \quad (2)$$

$$ClO_x^- + Re^{V}O_y \rightarrow ClO_{x-1}^- + Re^{VII}O_{y+1} \quad (3)$$

These findings affirm the opportunities for developing effective and sustainable water technologies with chemical innovation,[19] particularly the exploration of the periodic table. Notably, the oxide species of the other two Group 5 metals, niobium (Nb) and tantalum (Ta), have very different properties from V. For example, $NaNbO_3$ and $NaTaO_3$ are not water-soluble.[58] Generating aqueous Nb and Ta species requires excessive acid,[59] base,[60,61] or complexing agents.[62] Thus, integrating Nb and Ta with PGM catalysts via the add-and-use strategy is challenging and warrants future research efforts.

■ ASSOCIATED CONTENT

Supporting Information

The Supporting Information is available free of charge at https://pubs.acs.org/doi/10.1021/acs.est.3c06519.

Comparison with other catalysts; kinetic figures for the effects of V precursors, chlorate concentrations, and common inert anions; XPS spectra; calculated V speciation using Visual MINTEQ; details of electrochemical studies (PDF)

■ AUTHOR INFORMATION

Corresponding Authors

Jinyu Gao − *Department of Chemical and Environmental Engineering, University of California, Riverside, California 92521, United States;* orcid.org/0000-0002-1751-3430; Email: jgao034@ucr.edu, jinyu.gao001@gmail.com

Jinyong Liu − *Department of Chemical and Environmental Engineering, University of California, Riverside, California 92521, United States;* orcid.org/0000-0003-1473-5377; Email: jinyongl@ucr.edu, jinyong.liu101@gmail.com

Authors

Gongde Chen − *Department of Chemical and Environmental Engineering, University of California, Riverside, California 92521, United States*

Qi Fu − *Department of Chemical and Environmental Engineering, University of California, Riverside, California 92521, United States; MOE Key Laboratory of Bioinorganic and Synthetic Chemistry/KLGHEI of Environment and Energy Chemistry, School of Chemistry, Sun Yat-Sen University, Guangzhou, Guangdong 510275, China*

Changxu Ren − *Department of Chemical and Environmental Engineering, University of California, Riverside, California 92521, United States;* orcid.org/0000-0002-1109-794X

Cheng Tan − *Department of Chemical and Environmental Engineering, University of California, Riverside, California 92521, United States;* orcid.org/0000-0001-5878-6542

Haizhou Liu − *Department of Chemical and Environmental Engineering, University of California, Riverside, California 92521, United States;* orcid.org/0000-0003-4194-2566

Yin Wang − *Department of Civil and Environmental Engineering, University of Wisconsin-Milwaukee, Milwaukee, Wisconsin 53201, United States;* orcid.org/0000-0001-6723-7975

Complete contact information is available at: https://pubs.acs.org/10.1021/acs.est.3c06519

Author Contributions

J.G. conducted kinetic experiments, analyzed the data, and drafted the manuscript; G.C. and H.L. conducted electrochemical studies; Q.F. conducted kinetic experiments; C.R. assisted in XPS characterization; C.T. measured aqueous V concentrations; J.L. conceived the idea, conducted initial kinetic studies with Y.W., supervised the research, and revised the manuscript.

Notes

The authors declare no competing financial interest.

■ ACKNOWLEDGMENTS

Financial support was provided by the National Science Foundation (CBET-1932942 for J.G., C.R., and J.L.). Dr. Ich Tran assisted in the XPS characterization performed at the UC Irvine Materials Research Institute (IMRI) using instrumentation funded in part by the National Science Foundation Major Research Instrumentation Program (CHE-1338173).

■ REFERENCES

(1) *Expert Market Research. Global Sodium Chlorate Market Report and Forecast 2023−2028*; 2023. https://www.researchandmarkets.com/reports/5323457 (accessed October 22, 2023).

(2) Gorzalski, A. S.; Spiesman, A. L. Insights on chlorate occurrence, intra-system variability, and source water concentrations. *J. AWWA* **2015**, *107* (11), E613−E626.

(3) Cho, K.; Qu, Y.; Kwon, D.; Zhang, H.; Cid, C. m. A.; Aryanfar, A.; Hoffmann, M. R. Effects of anodic potential and chloride ion on overall reactivity in electrochemical reactors designed for solar-powered wastewater treatment. *Environ. Sci. Technol.* **2014**, *48* (4), 2377−2384.

(4) Jasper, J. T.; Yang, Y.; Hoffmann, M. R. Toxic byproduct formation during electrochemical treatment of latrine wastewater. *Environ. Sci. Technol.* **2017**, *51* (12), 7111−7119.

(5) Qian, Y.; Guo, X.; Zhang, Y.; Peng, Y.; Sun, P.; Huang, C.-H.; Niu, J.; Zhou, X.; Crittenden, J. C. Perfluorooctanoic acid degradation using UV−persulfate process: Modeling of the degradation and chlorate formation. *Environ. Sci. Technol.* **2016**, *50* (2), 772−781.

(6) Albolafio, S.; Marín, A.; Allende, A.; García, F.; Simón-Andreu, P. J.; Soler, M. A.; Gil, M. I. Strategies for mitigating chlorinated disinfection byproducts in wastewater treatment plants. *Chemosphere* **2022**, *288*, No. 132583.

(7) Vanwijk, D. J.; Hutchinson, T. H. The ecotoxicity of chlorate to aquatic organisms: A critical review. *Ecotoxicol. Environ. Saf.* **1995**, *32* (3), 244−253.

(8) Sutigoolabud, P.; Mizuno, T.; Ongprasert, S.; Karita, S.; Takahashi, T.; Obata, H.; Senoo, K. Effect of chlorate on nitrification in longan plantation soil. *Soil Sci. Plant Nutr.* **2008**, *54* (3), 387−392.

(9) Alfredo, K.; Stanford, B.; Roberson, J. A.; Eaton, A. Chlorate challenges for water systems. *J. AWWA* **2015**, *107* (4), 187.

(10) WHO *Chlorite and Chlorate in Drinking-Water: Background Document for Development of WHO Guidelines for Drinking-Water Quality; WHO/SDE/WSH/05.08/86*; World Health Organization, 2005.

(11) European Union Directive (EU) 2020/2184 of the European Parliament and of the Council of 16 December 2020 on the quality of water intended for human consumption (recast) (Text with EEA relevance). *Off. J. Eur. Union* **2020**, 1− 62.

(12) SAC *National standard of the People's Republic of China: standards for drinking water quality; GB 5749−2022*; Standardization Administration of China, 2022.

(13) EPA *Six-Year Review 3 Technical Support Document for Chlorate; EPA-810-R-16−013*; U.S. Environmental Protection Agency, Office of Water, 2016.
(14) U.S. Environmental. Protection Agency Revisions to the unregulated contaminant monitoring regulation (UCMR 3) for public water systems. *Fed. Regist.* **2012**, *77*, 26072−26101.
(15) Karlsson, R. K.; Cornell, A. Selectivity between oxygen and chlorine evolution in the chlor-alkali and chlorate processes. *Chem. Rev.* **2016**, *116* (5), 2982−3028.
(16) Lakshmanan, S.; Murugesan, T. The chlor-alkali process: Work in progress. *Clean Technol. Environ. Policy.* **2014**, *16* (2), 225−234.
(17) Park, H.; Vecitis, C. D.; Hoffmann, M. R. Electrochemical water splitting coupled with organic compound oxidation: The role of active chlorine species. *J. Phys. Chem. C* **2009**, *113* (18), 7935−7945.
(18) Kumar, A.; Phillips, K. R.; Thiel, G. P.; Schröder, U.; Lienhard, J. H. Direct electrosynthesis of sodium hydroxide and hydrochloric acid from brine streams. *Nat. Catal.* **2019**, *2* (2), 106.
(19) Liu, J.; Gao, J. Catalytic reduction of water pollutants: Knowledge gaps, lessons learned, and new opportunities. *Front. Environ. Sci. Eng.* **2022**, *17* (2), 26.
(20) Becker, A.; Koch, V.; Sell, M.; Schindler, H.; Neuenfeldt, G. Method of removing chlorate and bromate compounds from water by catalytic reduction. European Patent EP0779880B1, 1998.
(21) Van Santen, R.; Klesing, A.; Neuenfeldt, G.; Ottmann, A. Method for removing chlorate ions from solutions. U.S. Patent 6270682, 2001.
(22) Kuznetsova, L. I.; Kuznetsova, N. I.; Koscheev, S. V.; Zaikovskii, V. I.; Lisitsyn, A. S.; Kaprielova, K. M.; Kirillova, N. V.; Twardowski, Z. Carbon-supported iridium catalyst for reduction of chlorate ions with hydrogen in concentrated solutions of sodium chloride. *Appl. Catal., A: Gen.* **2012**, *427*, 8−15.
(23) Liu, J.; Chen, X.; Wang, Y.; Strathmann, T. J.; Werth, C. J. Mechanism and mitigation of the decomposition of an oxorhenium complex-based heterogeneous catalyst for perchlorate reduction in water. *Environ. Sci. Technol.* **2015**, *49* (21), 12932−12940.
(24) Chen, X.; Huo, X.; Liu, J.; Wang, Y.; Werth, C. J.; Strathmann, T. J. Exploring beyond palladium: Catalytic reduction of aqueous oxyanion pollutants with alternative platinum group metals and new mechanistic implications. *Chem. Eng. J.* **2017**, *313*, 745−752.
(25) Ye, T.; Banek, N. A.; Durkin, D. P.; Hu, M.; Wang, X.; Wagner, M. J.; Shuai, D. Pd nanoparticle catalysts supported on nitrogen-functionalized activated carbon for oxyanion hydrogenation and water purification. *ACS Appl. Nano Mater.* **2018**, *1* (12), 6580−6586.
(26) Liu, J.; Choe, J. K.; Sasnow, Z.; Werth, C. J.; Strathmann, T. J. Application of a Re−Pd bimetallic catalyst for treatment of perchlorate in waste ion-exchange regenerant brine. *Water Res.* **2013**, *47* (1), 91−101.
(27) Ren, C.; Yang, P.; Gao, J.; Huo, X.; Min, X.; Bi, E. Y.; Liu, Y.; Wang, Y.; Zhu, M.; Liu, J. Catalytic reduction of aqueous chlorate with MoO_x immobilized on Pd/C. *ACS Catal.* **2020**, *10* (15), 8201−8211.
(28) Gao, J.; Zhao, Q.; Tan, C.; Xie, S.; Yin, Y.; Liu, F.; Liu, H.; Chen, B.; Liu, J. Accelerating catalytic oxyanion reduction with inert metal hydroxides. *Environ. Sci. Technol.* **2023**, *57* (3), 1479−1486.
(29) Gao, J.; Xie, S.; Liu, F.; Liu, J. Preparation and synergy of supported Ru^0 and Pd^0 for rapid chlorate reduction at pH 7. *Environ. Sci. Technol.* **2023**, *57* (9), 3962−3970.
(30) Hurley, K. D.; Shapley, J. R. Efficient heterogeneous catalytic reduction of perchlorate in water. *Environ. Sci. Technol.* **2007**, *41* (6), 2044−2049.
(31) Langeslay, R. R.; Sattelberger, A. P.; Marshall, C. L.; Kaphan, D. M.; Delferro, M.; Stair, P. C. Catalytic applications of vanadium: A mechanistic perspective. *Chem. Rev.* **2019**, *119* (4), 2128−2191.
(32) Galloni, P.; Conte, V.; Floris, B. A journey into the electrochemistry of vanadium compounds. *Coord. Chem. Rev.* **2015**, *301−302*, 240−299.
(33) Choi, C.; Kim, S.; Kim, R.; Choi, Y.; Kim, S.; Jung, H.-y.; Yang, J. H.; Kim, H.-T. A review of vanadium electrolytes for vanadium redox flow batteries. *Renew. Sustain. Energy Rev.* **2017**, *69*, 263−274.
(34) Cotton, A. F.; Wilkinson, G.; Murillo, C. A.; Bochmann, M. *Advanced Inorganic Chemistry*; Wiley, 1999.
(35) Shiller, A. M.; Mao, L. Dissolved vanadium in rivers: Effects of silicate weathering. *Chem. Geol.* **2000**, *165* (1), 13−22.
(36) Schlesinger, W. H.; Klein, E. M.; Vengosh, A. Global biogeochemical cycle of vanadium. *Proc. Natl. Acad. Sci. U.S.A.* **2017**, *114* (52), E11092−E11100.
(37) Watt, J. A. J.; Burke, I. T.; Edwards, R. A.; Malcolm, H. M.; Mayes, W. M.; Olszewska, J. P.; Pan, G.; Graham, M. C.; Heal, K. V.; Rose, N. L.; Turner, S. D.; Spears, B. M. Vanadium: A re-emerging environmental hazard. *Environ. Sci. Technol.* **2018**, *52* (21), 11973−11974.
(38) Zhang, B.; Wang, S.; Diao, M.; Fu, J.; Xie, M.; Shi, J.; Liu, Z.; Jiang, Y.; Cao, X.; Borthwick, A. G. L. Microbial community responses to vanadium distributions in mining geological environments and bioremediation assessment. *J. Geophys. Res. Biogeosci.* **2019**, *124* (3), 601−615.
(39) Gao, J.; Ren, C.; Huo, X.; Ji, R.; Wen, X.; Guo, J.; Liu, J. Supported palladium catalysts: A facile preparation method and implications to reductive catalysis technology for water treatment. *ACS ES&T Eng.* **2021**, *1* (3), 562−570.
(40) Ren, C.; Bi, E. Y.; Gao, J.; Liu, J. Molybdenum-catalyzed perchlorate reduction: Robustness, challenges, and solutions. *ACS ES&T Eng.* **2022**, *2* (2), 181−188.
(41) Chen, G.; Liu, H. Understanding the reduction kinetics of aqueous vanadium(V) and transformation products using rotating ring-disk electrodes. *Environ. Sci. Technol.* **2017**, *51* (20), 11643.
(42) Ren, C.; Yang, P.; Sun, J.; Bi, E. Y.; Gao, J.; Palmer, J.; Zhu, M.; Wu, Y.; Liu, J. A bioinspired molybdenum catalyst for aqueous perchlorate reduction. *J. Am. Chem. Soc.* **2021**, *143* (21), 7891−7896.
(43) Bruyère, V. I. E.; García Rodenas, L. A.; Morando, P. J.; Blesa, M. A. Reduction of vanadium(V) by oxalic acid in aqueous acid solutions. *J. Chem. Soc., Dalton Trans.* **2001**, 3593−3597.
(44) Michibata, H.; Yamaguchi, N.; Uyama, T.; Ueki, T. Molecular biological approaches to the accumulation and reduction of vanadium by ascidians. *Coord. Chem. Rev.* **2003**, *237*, 41−51.
(45) Silversmit, G.; Depla, D.; Poelman, H.; Marin, G. B.; De Gryse, R. Determination of the V2p XPS binding energies for different vanadium oxidation states (V^{5+} to V^{0+}). *J. Electron. Spectrosc. Related Phenom.* **2004**, *135*, 167−175.
(46) Hryha, E.; Rutqvist, E.; Nyborg, L. Stoichiometric vanadium oxides studied by XPS. *Surf. Interface Anal.* **2012**, *44*, 1022−1025.
(47) Boukhobza, I.; Crans, D. C. Application of HPLC to measure vanadium in environmental, biological and clinical matrices. *Arab. J. Chem.* **2020**, *13* (1), 1198−1228.
(48) Bard, A. J.; Faulkner, L. R. *Electrochemical methods: fundamentals and applications*. 2nd ed.; Wiley: New York, 2000.
(49) Cornelius, R. D.; Gordon, G. Kinetics and mechanism of the oxidation of vanadium (III) by chlorate ion, chlorine dioxide, chlorous acid, and hypochlorous acid. *Inorg. Chem.* **1976**, *15* (5), 1002−1006.
(50) Melvin, W. S.; Gordon, G. Mechanism of inhibition of the vanadium (IV)-chlorate reaction by chloride ion. *Inorg. Chem.* **1972**, *11* (8), 1912−1917.
(51) Buglyó, P.; Crans, D. C.; Nagy, E. M.; Lindo, R. L.; Yang, L.; Smee, J. J.; Jin, W.; Chi, L.-H.; Godzala, M. E.; Willsky, G. R. Aqueous chemistry of the vanadium^{III} (V^{III}) and the V^{III}−dipicolinate systems and a comparison of the effect of three oxidation states of vanadium compounds on diabetic hyperglycemia in rats. *Inorg. Chem.* **2005**, *44* (15), 5416−5427.
(52) King, W. R., Jr.; Garner, C. S. The exchange of vanadium(II) and vanadium(III) ions in perchloric and sulfuric acid solutions. *J. Am. Chem. Soc.* **1952**, *74* (14), 3709−3710.
(53) Huang, J.-H.; Huang, F.; Evans, L.; Glasauer, S. Vanadium: Global (bio)geochemistry. *Chem. Geol.* **2015**, *417*, 68−89.
(54) Imtiaz, M.; Rizwan, M. S.; Xiong, S.; Li, H.; Ashraf, M.; Shahzad, S. M.; Shahzad, M.; Rizwan, M.; Tu, S. Vanadium, recent advancements and research prospects: A review. *Environ. Int.* **2015**, *80*, 79−88.

https://doi.org/10.1021/acs.est.3c06519
Environ. Sci. Technol. 2023, 57, 20392−20399

(55) Graedel, T. E.; Miatto, A. Vanadium: A U.S. Perspective on an understudied metal. *Environ. Sci. Technol.* **2023**, *57* (24), 8933−8942.
(56) Cao, X.; Diao, M.; Zhang, B.; Liu, H.; Wang, S.; Yang, M. Spatial distribution of vanadium and microbial community responses in surface soil of panzhihua mining and smelting area, china. *Chemosphere* **2017**, *183*, 9−17.
(57) Wang, S.; Zhang, B.; Li, T.; Li, Z.; Fu, J. Soil vanadium(V)-reducing related bacteria drive community response to vanadium pollution from a smelting plant over multiple gradients. *Environ. Int.* **2020**, *138*, No. 105630.
(58) Ozmen, O.; Ozsoy-Keskinbora, C.; Suvaci, E. Chemical stability of $KNbO_3$, $NaNbO_3$, and $K_{0.5}Na_{0.5}NbO_3$ in aqueous medium. *J. Am. Ceram. Soc.* **2018**, *101* (3), 1074−1086.
(59) Kanzelmeyer, J. H.; Ryan, J.; Freund, H. The nature of niobium(V) in hydrochloric acid solution[1]. *J. Am. Chem. Soc.* **1956**, *78* (13), 3020−3023.
(60) Kennedy, J. H. Sodium-potassium niobates and tantalates. *J. Inorg. Nucl. Chem.* **1961**, *20* (1), 53−57.
(61) Deblonde, G. J. P.; Chagnes, A.; Bélair, S.; Cote, G. Solubility of niobium(V) and tantalum(V) under mild alkaline conditions. *Hydrometallurgy* **2015**, *156*, 99−106.
(62) Fairbrother, F.; Robinson, D.; Taylor, J. B. Some water-soluble complexes of pentavalent niobium and tantalum. *J. Inorg. Nucl. Chem.* **1958**, *8*, 296−301.

https://doi.org/10.1021/acs.est.3c06519
Environ. Sci. Technol. 2023, 57, 20392−20399